Proceedings of 2001 Korea-Japan Joint Seminar
on Particle Image Velocimetry
Seoul National Univ., Dec. 3 - 4

Effect of lock-on frequency on vortex shedding in the cylinder wake

Jung Yul Yoo*, Jaeyong Sung**, Wontae Kim*

*School of Mechanical and Aerospace Engineering, Seoul National University
Seoul 151-742, Korea
**LG Electronics, Inc., 327-23 Gasan-dong, Keumchun-gu, Seoul 153-802, Korea

Abstract

Vortex lock-on or resonance in the flow behind a circular cylinder is investigated from a time-resolved PIV when a single frequency oscillation is superimposed on the mean incident velocity. Measurements are made of the Kármán and streamwise vortices in the wake-transition regime at the Reynolds number 360. Streamwise vortices at the lock-on and natural shedding states are observed, as well as the changes in the wake region with the change of the shedding frequency of lock-on state. When lock-on occurs, the vortex shedding frequency is found to be half the oscillation frequency as expected from previous experiments. At the lock-on state, the Kármán vortices are observed to be more disordered by the increased strength and spanwise wavelength of the streamwise vortices, which leads to a strong three-dimensional motion. Recirculation and vortex formation region at the lock-on state is reduced as the oscillating frequency is increased. By comparing the Reynolds stresses at the lock-on and natural shedding states, $\overline{u'u'}$ and $\overline{u'v'}$ at the lock-on state are concentrated on the shear layer around the cylinder. The $\overline{v'v'}$ at f_o/f_n =2.0 has a large value near the centerline, compared with that of other cases. Considering the traces of maximum of u', in the wake region near the cylinder, wake width at the lock-on state is wider than that at the natural shedding state.

Keyword: Lock-on, Oscillatory Flow, Streamwise Vortex, Time-Resolved PIV, Reynolds stress

1. Introduction

Over the past decade, a considerable amount of work has been carried out on the coherent structures in the near wake of a circular cylinder for laminar, transitional and turbulent flows. They have been constantly of great research interest because even at low Reynolds numbers, of the order of a few hundred, the flow has three-dimensional structures. Until the shear layer vortices are formed at the Reynolds number above 1000, the flow field is refered to as wake-transition regime, where the secondary vortices with the spanwise wavelength of about one

cylinder diameter appear (Williamson, 1996). Considering that three-dimensionality is introduced in the near-wake region by some flow instability, it is of great importance to observe the topological features of the structures in this region.

Vortex shedding from bluff bodies has been one of the most important problems in the design of structures since it gives rise to fluctuating lift and drag forces acting on the body. In particular, when a bluff cylinder is excited into resonant oscillations by an incident flow, there is a substantial increase not only in the oscillatory lift force but also in the mean drag force, which may cause the failure of bluff structures (Armstrong *et al.*, 1986). This resonance between the vortex shedding and oscillation frequency is commonly termed as lock-on. According to an extensive review given by Griffin & Hall (1991), vortex resonance, or lock-on, has been observed also when a cylinder was forced to oscillate circumferentially, or in the direction normal to, or in-line with the incident flow. It is known that in case of the cross-flow and rotational oscillations, lock-on occurs when the oscillation frequency is near the natural shedding frequency. On the other hand, as for the oscillatory flow and in-line oscillation, the resonant frequency is twice the natural frequency because the forcing is given in the same direction as the fluctuating drag force, of which the frequency is twice the shedding frequency. But the primary interest of the present study is in the flow-induced resonance, which has drawn less attention than other types of oscillation. The flow phenomenon is encountered in numerous engineering applications such as civil engineering, power generation, turbomachinery, etc., notwithstanding their physical importance (Hall & Griffin, 1993).

There have been several investigations of the locked-on wakes. The first observation of lock-on was made by Barbi *et al.* (1986) in the case of a fixed cylinder subject to an oscillatory incident flow with non-zero mean velocity. They found that the vortex shedding was synchronized with the oscillation frequency in a range of frequencies near twice the natural shedding frequency, which was similar to the in-line oscillation of a cylinder. Earlier, Hatfield & Morkovin (1973) attempted to study the same problem, but their results were inconclusive because the oscillation amplitude and frequency were too low to cause lock-on. Armstrong *et al.* (1986) examined the effects of an oscillatory flow on the flow over three bluff bodies, a circular cylinder, a flat plate and a D-section. They reported that the lock-on range increased and the minimum base pressure decreased as the oscillation amplitude increased. As an extension of the above study, they also compared the turbulent wake in the steady flow with that in the oscillatory flow where lock-on took place (Armstrong *et al.*, 1987). The conditionally averaged flow fields were measured 7-diameter downstream of the cylinder using a traversing cross-wire. Their results showed that with lock-on, the Kármán vortices had an increased strength and a decreased lateral separation although the time-mean wake velocity profile did not change. Meanwhile, Hall & Griffin (1993) fulfilled computational works at the Reynolds number 200 and presented that the vortex formation region, of which the end was defined as a peak position

in the rms velocity fluctuation along the centerline, varied inversely with the oscillation frequency in the lock-on regime and was reduced in length by increasing the amplitude of oscillation.

The present study is focused on streamwise vortices and phase-averaged structures under lock-on state of the oscillatory flow as well as the effect of lock-on frequency in comparison with those in the steady flow. Using a time-resolved PIV system, the three-dimensional flow fields are measured in the wake-transition regime at the Reynolds number 360. For this purpose, the region of recirculation and vortex formation, Reynolds stress and maximum of u' are estimated.

2. Experimental arrangement

Figure 1 shows experimental setup. Measurements are made in a closed-circuit water tunnel with the size of the test section, which is 15 cm wide, 10 cm high and 100 cm long. A circular cylinder is made of an acrylic plastic bar and placed horizontally across the test section, which is 5 mm in diameter D, giving an aspect ratio of 30. The coordinate system is defined such that the origin is located at the center of the circular cylinder with x, y and z representing the streamwise, cross-stream (transverse) and spanwise directions, respectively. The flow oscillation is produced by rotating a set of three shutters that are located at the downstream end of the working section (Armstrong *et al.* 1986). Each of the shutters comprises pairs of rectangular steel plates that fit into three vertical stainless-steel rods which are spaced at equal distances. The shutters are rotated in phase by a variable AC servo-motor through a timing-belt drive. The frequency of the velocity oscillation f_o is twice that of the shutters since the time-varying blockage imposed on the flow by the shutters, repeats itself every half turn of the shutters. This system for producing an oscillatory flow is similar to that described by Armstrong *et al.* (1986). According to Al-Asmi & Castro (1993), there have been several devices to generate oscillatory flows. The most popular way is to use downstream devices such as rotating vanes, valves or shutters. An obvious advantage of this technique is that sinusoidal waveforms with acceptable purity can be induced and much higher frequency oscillations can be generated than is possible with other techniques. However, large fluctuating static pressure in the test section is inevitable, since it drives the velocity fluctuation. Some workers have installed similar devices at positions upstream of the test section. This technique has a merit of small fluctuating static pressure, compared with the downstream devices, but may lead to higher levels of free-stream turbulence. Although there are several other techniques such as oscillating flaps and flow bypass techniques to avoid large pressure discontinuities, these also have a disadvantage of poor cross-sectional uniformity and nearly sinusoidal waveform. It is known that the oscillating amplitude affects the frequency limit of the lock-on (Barbi *et al.*, 1986) but further

consideration is not made in the present study. The variations of the free-stream velocity by the presence of the oscillating shutters are less than 1%. The non-dimensional amplitude of the free-stream turbulence is about 0.002, which is too low to affect locked-on structures.

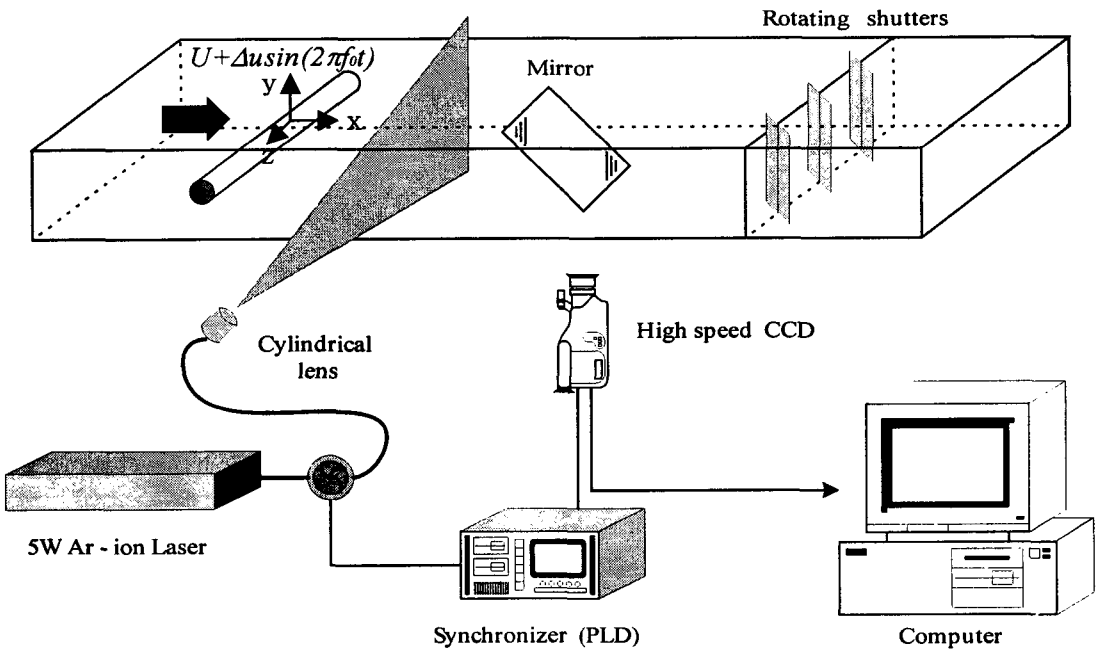

Fig. 1 Experimental set-up for producing an oscillatory flow and measuring the flow field with a time-resolved PIV system

To measure the streamwise vortices, an image-reflecting mirror oriented at 45° is located far downstream ($x/D > 40$) of the cylinder ensuring that the placement of the mirror does not affect the near wake of the cylinder, which is the region of primary interest. The vortex shedding from a circular cylinder in steady and oscillatory flows is measured in the wake-transition regime at the Reynolds number 360. The fields of view are $0 < x < 4.6D$ and $-2D < y < 2D$ in the x-y plane, and $-1.5D < y < 1.5D$ and $0 < z < 3.4D$ in the y-z plane. The three-dimensional near wake of a circular cylinder is measured by a time-resolved PIV system (Sung & Yoo, 2001). Velocity vectors are determined by cross-correlation analysis using FFT's with 16-pixel × 16-pixel interrogation windows through a super-resolution processing (Hart, 2000).

3. Results and Discussion

3.1 Flow characteristics in the wake-transition regime

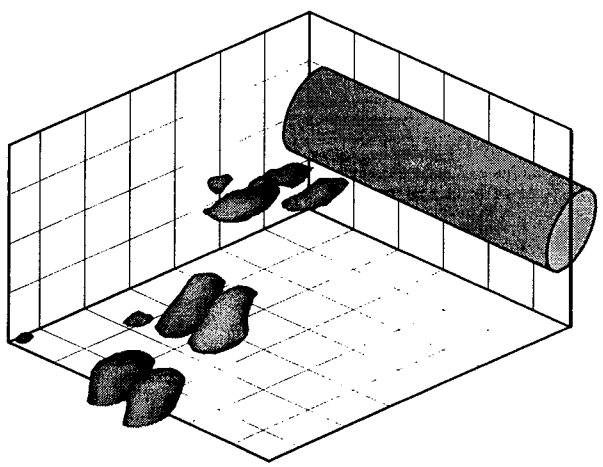

Fig. 2 Iso-vorticity surfaces of the secondary vortex. The left and right surfaces correspond to $\omega_y/(U/D) = 0.15$ and - 0.15, respectively.

First of all, the steady flow in the near-wake of the cylinder is investigated. This will help to easily understand the change of structure by lock-on in wake-transition regime. This flow regime has three-dimensional characteristics. A detailed description of the temporal behavior of the three-dimensional structure can be found in our previous work (Sung & Yoo, 2001). Here, we only recall the reconstructed flow field for further analysis on flow topology in the near wake. Figure 2 shows the three-dimensional dispositions of the secondary vortices at phase 0°, which are forming a vortex filament. In this plot, the left and right iso-vorticity surfaces of the secondary vortices, which represent positive and negative values, respectively, configure to a vortex pair counter-rotating with respect to each other.

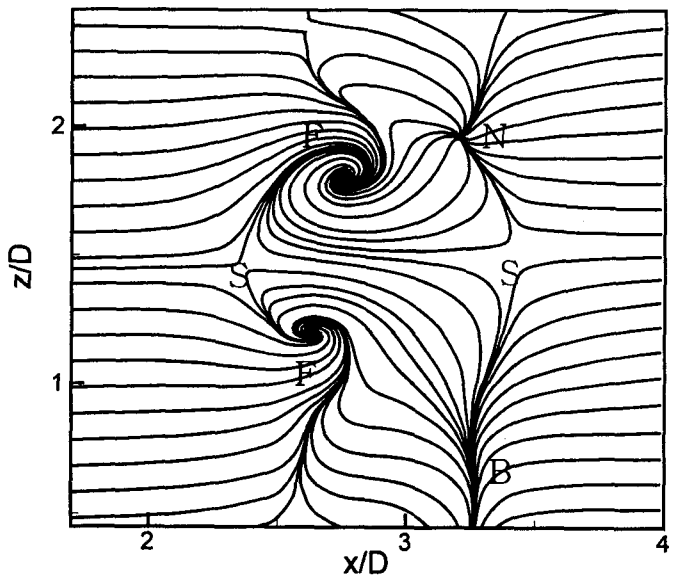

Fig. 3 Streamlines in the z-x plane at y/D = - 0.5, viewed from a moving frame of reference at phase 0°: S, saddle; F, focus; N, node; B, bifurcation line.

Examining the z-x plane, the streamline pattern of Figure 3 shows the existence of a node and a bifurcation line as well as the foci and saddles. Among those, a bifurcation line occurs when critical points merge, spilt or change type as their trajectories cross the boundaries between topological domains (Chong *et al.*, 1990). Another interesting feature in the z-x plane is that the sectional streamlines describe well the mushroom-type structures frequently seen in previous flow visualization (Williamson, 1996).

In the x-y plane, the saddle from Figure 4 seems to be located just upstream of the secondary vortices when one considers a plane normal to the page and containing the saddle. Thus, the spanwise position of the saddle in Figure 4 is thought to approximately coincide with that of the upstream saddle of the secondary vortices in Figure 3. The schematic model in Figure 5, representing streamlines around a saddle in a frame of reference moving with the vortices, shows that one diverging separatrix of a saddle squeezes the filaments while they are stretched in the opposite directions along another diverging separatrix.

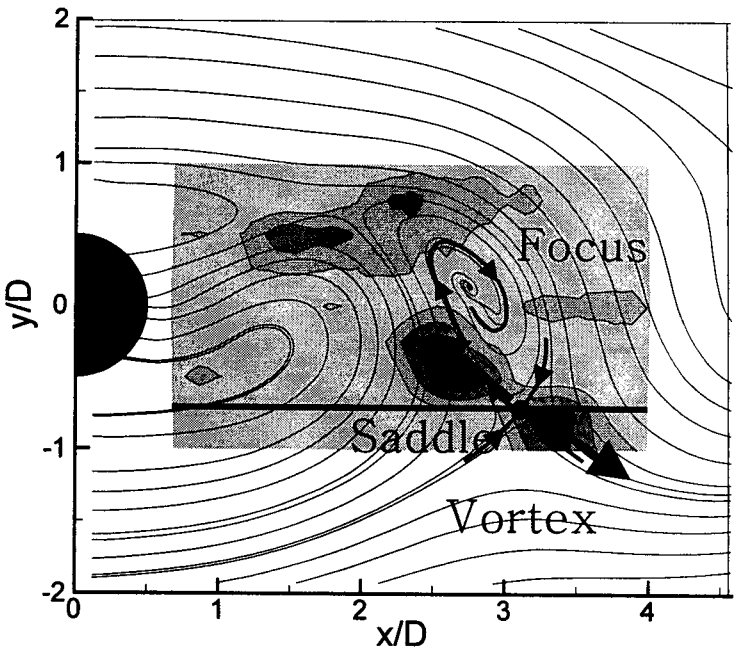

Fig. 4 Streamlines and vorticity contours of the secondary vortex (ω_y) at phase 0° viewed from a moving frame of reference

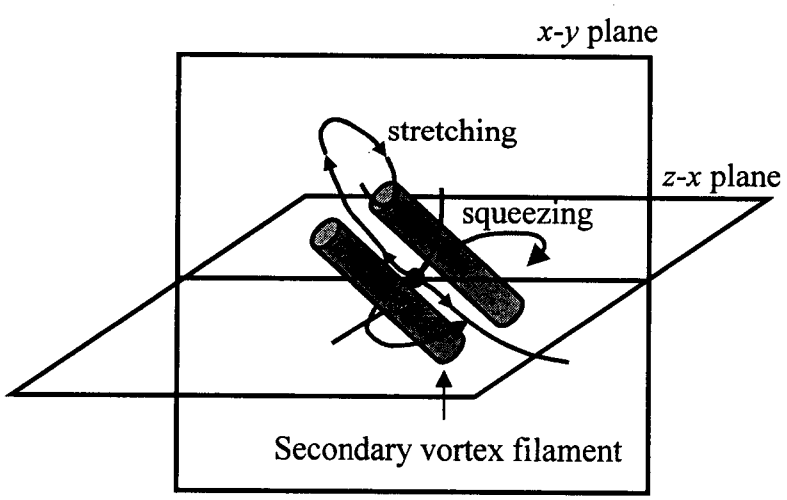

Fig. 5 Schematic model of the three-dimensional streamlines around a saddle. There are two diverging separatrices. One of them stretches vortex filament and the other squeezes the filament.

3.2 Streamwise vortices & phase-averaged structures under lock-on state and natural shedding

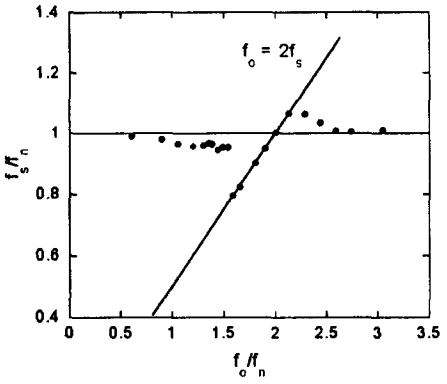

Fig. 6 Frequency response of vortex shedding according to oscillation frequency

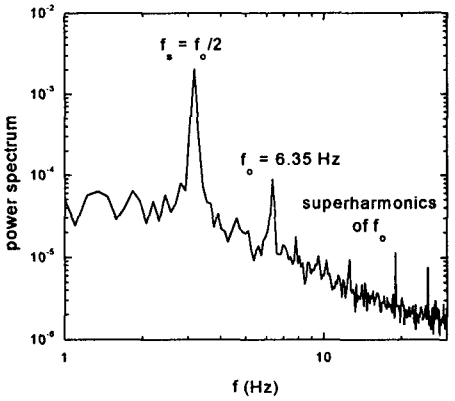

Fig. 7 Power spectrum of the velocity signal in the lock-on state, $f_o/f_n = 2.0$

For constant free-stream velocity, measurements are made of the vortex shedding frequency f_s from the cylinder as the oscillation frequency is varied. Figure 6 shows the variations of the shedding frequency with the oscillation frequency f_o, where the natural shedding frequency f_n is defined as a shedding frequency in steady incident flow condition. In this figure, the shedding frequency is determined by power spectra of the streamwise velocity signal at (x/D, y/D) = (1.5, -0.5). It appears clearly that the shedding frequency is locked-on to the oscillation frequency over a range of oscillation frequency ($1.5 < f_o/f_n < 2.2$). Note that vortex lock-on usually occurs near twice the natural shedding frequency. Figure 7 shows power spectrum for lock-on state, $f_o/f_n = 2.0$. During lock-on, the ratio f_s/f_o is kept at 0.5, which agrees well with the previous results of Barbi et al. (1986). When a bluff cylinder is excited into resonant oscillations by an incident flow, the characteristics of the near-wake flow are changed. In the present study, the lock-on is investigated in a phase-averaged sense. Figure 8 shows the phase-averaged Kármán vortices in the x-y plane for the steady and lock-on conditions. In this figure, it seems that the Kármán vortices under the lock-on condition are more dissipative than those under the steady condition. On the other hand, this may be mainly caused by the cycle-to-cycle variations of the Kármán vortex formation due to strong three-dimensional motions.

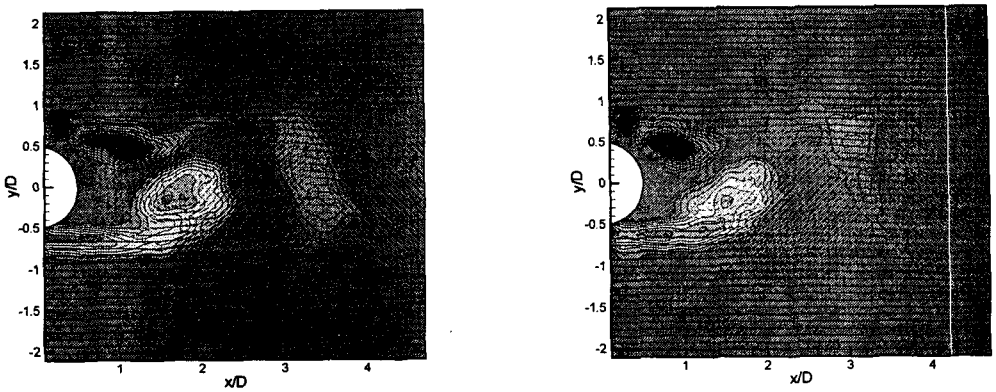

(a) (b)

Fig. 8 Phase-averaged Kármán vortices in the x-y plane for (a) natural shedding and (b) locked-on shedding

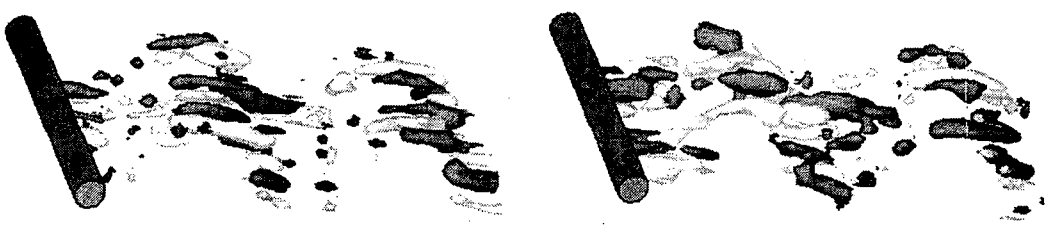

(a) (b)

Fig. 9 Spatio-temporal representations of the streamwise vortices in the y-z plane at x/D = 2.5 for (a) natural shedding and (b) locked-on shedding

In the wake-transition regime of the present Reynolds number, the three-dimensional wake is characterized by the secondary vortices with a spanwise length scale of about one diameter. Thus, it is of great importance to interpret the spatio-temporal evolutions of streamwise vortices. The spatio-temporal representations of Figure 9 show iso-vorticity surfaces of the streamwise vorticity in the steady and lock-on conditions. The streamwise coordinate is proportional to Ut. Considering the overall shape of the vorticity pattern, it exhibits a large-scale undulation for the two conditions due to successive formation of the Kármán vortices. However, the streamwise vortices are different in strength and length scale. At a given cross-section of a vorticity field, it is possible to evaluate the magnitude of the streamwise circulation Γ_x. The time-averaged value is $|\Gamma_x|/\pi UD = 11.87 = 11.87$ for the steady condition, while it is 15.82 for the lock-on condition, giving rise to a 33% increase. The spanwise wavelength can be also obtained from the spatial correlation of the instantaneous vorticity distributions. The averaged wavelength is found to be $0.93D$ and $1.18D$ for the steady and lock-on conditions, respectively, which corresponds to a 27% increase by the lock-on.

3.3 Effect of shedding frequency of the lock-on state

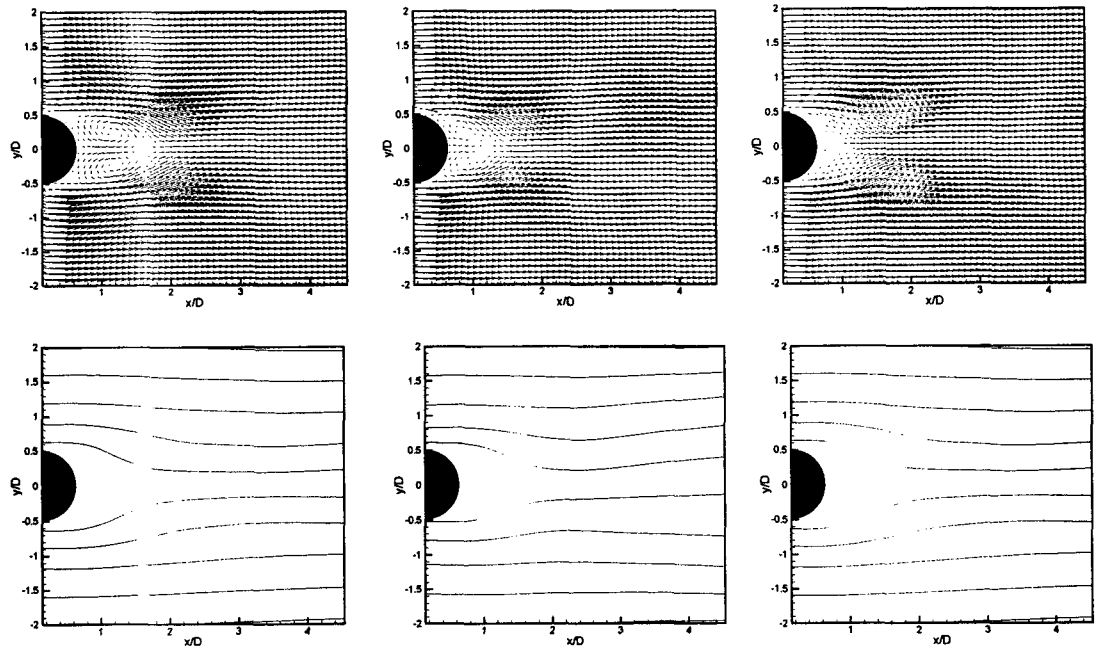

(a) f_o/f_n =0 (b) f_o/f_n =1.6 (c) f_o/f_n =2.0

Fig. 10 Mean velocity and streamlines

The flow is measured for three cases (f_o/f_n = 0 of natural shedding, f_o/f_n =1.6 and 2.0 of lock-on states). In Figure 10, time-averaged velocity fields and streamlines are shown. As for time-averaged velocity fields, it is observed that the recirculation region at the lock-on states is shorter than that in the natural shedding state. Meanwhile, comparing the streamline pattern of f_o/f_n =2.0 with that of the natural shedding state, there is a similar trend in the streamline curvature downstream of the recirculation region. But, for f_o/f_n =1.6, the shedding is weak and streamline spacings become wider as we move downstream.

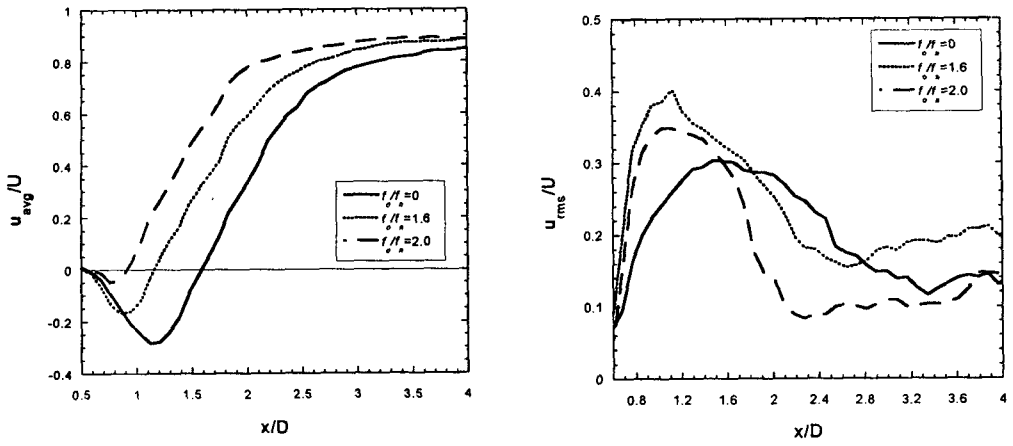

(a) (b)

Fig. 11 Comparison of (a) the long-time averaged centerline velocity and (b) rms velocity fluctuation for the natural shedding and lock-on states which are f_o/f_n = 1.6 and 2.0, respectively

In Figure 11(a), mean velocity in the x-direction along the wake centerline is shown. As forcing oscillation frequency is increased, the recirculation region is reduced.

The cylinder base-region flow in the vortex formation region is important to the development of the near wake flow (Bearman, 1965), (Gerrard, 1966), and to the ensuing physical evolution of the wake. One measure of the downstream extent of the formation region is the maximum in the fluctuating velocity which occurs just downstream of the cylinder along the wake centerline (Hall, 1993). In Figure 11(b), the rms fluctuation of streamwise velocity along the wake centerline is shown. The peak for u_{rms} related vortex formation region is located at about 1.0D, 1.1D and 1.6D for f_o/f_n =0, 1.6 and 2.0, respectively. These values are nearly the same as the dimensionless recirculation length. The peak value of the u' at the lock-on condition is greater than that for natural shedding, as shown in Figure 11(b). Therefore, it is obvious that the regions of vortex formation and recirculation are reduced by the locked-on vortex shedding, which agrees with the previous work (Griffin & Hall, 1991).

Figure 12 shows the distributions of the Reynolds stresses, $\overline{u'u'}$, $\overline{u'v'}$ and $\overline{v'v'}$ of all cases, where the instantaneous velocity, u is decomposed into time-mean component, $\bar{u}$ and fluctuating component, u'. There is some distinction in the Reynolds stress between natural shedding and lock-on conditions. First, as for the $\overline{u'u'}$, it is found that $\overline{u'u'}$ of lock-on state has high value in top and bottom shear layers, compared with the natural shedding state. It seems that in the lock-on state $\overline{u'u'}$ is concentrated on the shear layer around the cylinder. Second, as for the $\overline{u'v'}$, it is seen that like the $\overline{u'u'}$ it is also concentrated on the shear layer of the cylinder. However, $\overline{u'v'}$ for f_o/f_n=1.6 has a broader region, compared with that for f_o/f_n=2.0.

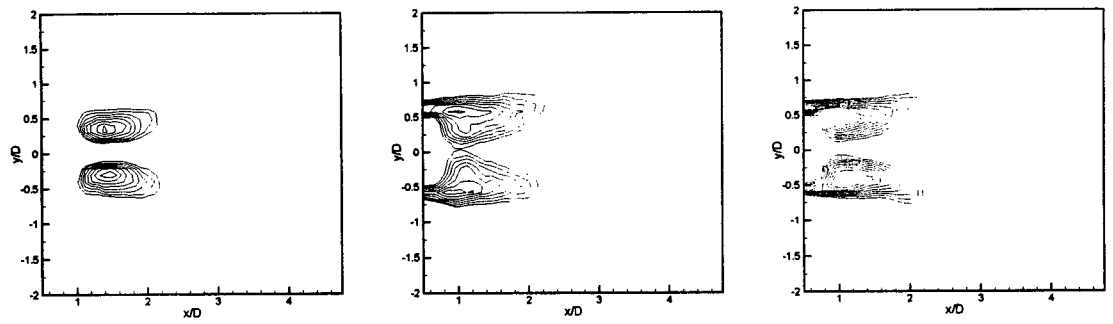

(a) $\overline{u'u'}$ for $f_o/f_n = 0$ (b) $\overline{u'u'}$ for $f_o/f_n = 1.6$ (c) $\overline{u'u'}$ for $f_o/f_n = 2.0$

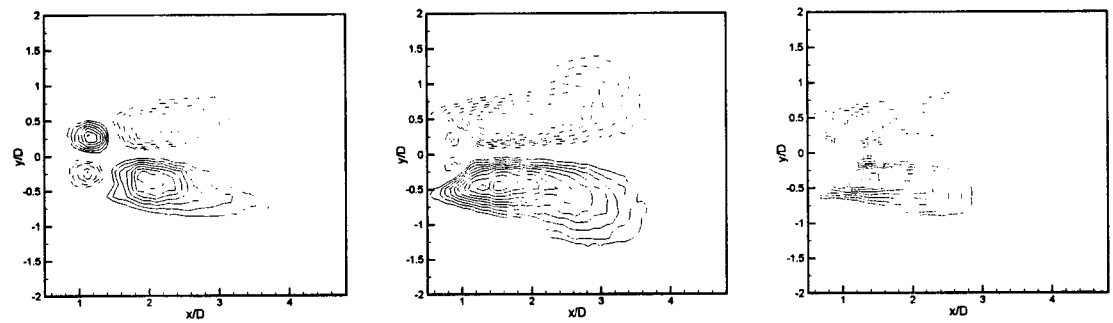

(d) $\overline{u'v'}$ for $f_o/f_n = 0$ (e) $\overline{u'v'}$ for $f_o/f_n = 1.6$ (f) $\overline{u'v'}$ for $f_o/f_n = 2.0$

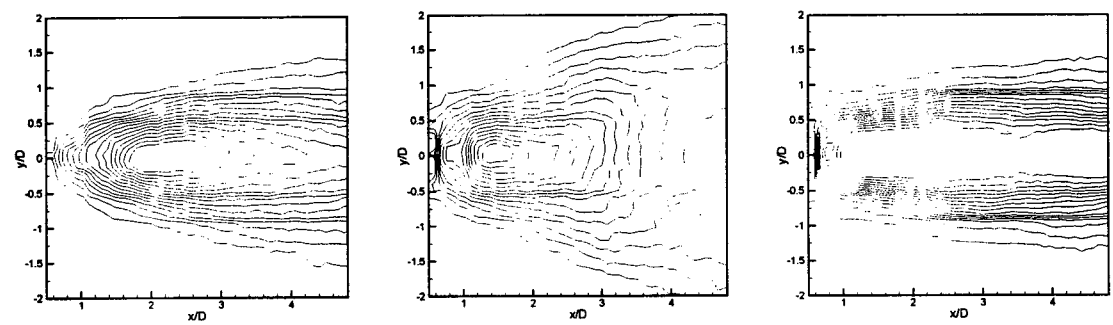

(g) $\overline{v'v'}$ for $f_o/f_n = 0$ (h) $\overline{v'v'}$ for $f_o/f_n = 1.6$ (i) $\overline{v'v'}$ for $f_o/f_n = 2.0$

Fig. 12 Reynolds stresses, $\overline{u'u'}$, $\overline{u'v'}$ and $\overline{v'v'}$

The $\overline{u'u'}$ and $\overline{u'v'}$ of the lock-on state are concentrated on the shear layer around the cylinder. This indicates that the cylinder is subject to severer variation of force at the lock-on state. Third, the $\overline{v'v'}$ of all three cases commonly have peak on the centerline. The starting point of peak range of lock-on is closer to the backside of the cylinder than that of natural shedding. The $\overline{v'v'}$ of the shedding motion at f_o/f_n =2.0 has a large value near the centerline, compared with that of other cases.

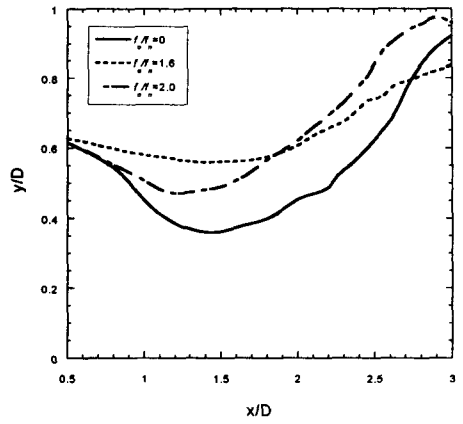

Fig. 13 Trace of maximum of u'

Figure 13 shows trace of maximum of u'. In the near-wake of 0.5 < x/D <3, wake width for the lock-on state is wider than that for the natural shedding state. It is indicated that the perturbation of the flow affects the fluctuation of downstream velocity. The wake region corresponding to f_o/f_n = 1.6 becomes wider in the near field, but that corresponding to f_o/f_n = 2.0 becomes even wider in the far field.

4. Concluding Remarks

The occurrence of lock-on is demonstrated by presenting the relationship that the shedding frequency is half the oscillation frequency. When lock-on takes place, stronger three-dimensional motion is induced, which makes the phase-averaged Kármán vortices appear to be more dissipative. From the spatio-temporal representations of the streamwise vortices, significant emphasis is placed on the increased strength and spanwise wavelength of the streamwise vortices at the lock-on.

The recirculation and vortex formation region at the lock-on state are shorter than those at the natural shedding state. As the frequency of the lock-on state is increased, the recirculation and vortex formation region is reduced. By comparing the Reynolds stresses at the lock-on and natural shedding states, $\overline{u'u'}$ and $\overline{u'v'}$ at the lock-on state are concentrated on the shear layer around the cylinder. The $\overline{v'v'}$ at f_o/f_n = 2.0 has a large value near the centerline, compared with that of other cases. Considering the traces of maximum of u', in the wake region near the cylinder, wake width at the lock-on state is wider than that at the natural shedding state.

References

[1] Al-Asmi, K. and Castro, I. P., "Production of oscillatory flow in wind tunnels", *Exp. Fluids*, Vol. 15, (1993), pp. 33-41.

[2] Armstrong, B. J., Barnes, F. H. and Grant, I., "The effect of a perturbation on the flow over a bluff cylinder", *Phys. Fluids*, Vol. 29, No. 7, (1986), pp. 2095-2102.

[3] Armstrong, B. J., Barnes, F. H. and Grant, I., "A comparison of the structure of the wake behind a circular cylinder in a steady flow with that in a perturbed flow", *Phys. Fluids*, Vol. 30, No. 1, (1987), pp. 19-26.

[4] Barbi, C., Favier, D. P., Maresca, C. A. and Telionis, D. P., "Vortex shedding and lock-on of a circular cylinder in oscillatory flow", *J. Fluid Mech.*, Vol. 170, (1986), pp. 527-544.

[5] Bearman, P. W., "Investigation of the flow behind a two dimensional model with a blunt trailing edge and fitted with splitter plates", *J. Fluid Mech.*, Vol. 16, (1965), pp. 241-255.

[6] Chong, M. S., Perry, A. E. and Cantwell, B. J., "A general classification of three-dimensional flow fields", *Phys. Fluids A*, Vol. 2, No. 5, (1990), pp. 765-777.

[7] Gerrard, J. H., "The mechanics of the formation region of vortices behind bluff bodies", *J. Fluid Mech.*, Vol. 25, (1966), pp. 461-489.

[8] Griffin, O. M. and Hall, M. S., "Review - Vortex shedding lock-on and flow control in bluff body wakes", *ASME J. Fluids Engrg.*, Vol. 113, (1991), pp. 526-537.

[9] Hall, M. S., "Vortex shedding and lock-on in a perturbed flow", *J. Fluids Engng.*, Vol. 115, No. 6, (1993), pp. 283-291.

[10] Hall, M. S. and Griffin, O. M., "Vortex shedding and lock-on in a perturbed flow", *ASME J. Fluids Engrg.*, Vol. 115, (1993), pp. 283-291.

[11] Hart, D. P., "PIV error correction", *Exp. Fluids*, Vol. 29, (2000), pp. 13-22.

[12] Hatfield, H. M. and Morkovin, M. V., "Effect of an oscillating free stream on the unsteady pressure on a circular cylinder", *ASME J. Fluids Engrg.*, Vol. 95, (1973), pp. 249-254.

[13] Sung, J. and Yoo, J. Y., "Three-dimensional phase-averaging of time-resolved PIV measurement data", *Meas. Sci. Tech.*, (2001), to appear.

[14] Williamson, C. H. K., "Three-dimensional wake transition", *J. Fluid Mech.*, Vol. 328, (1996), pp. 345-407.